

# Effects of core degrees of freedom in the low energy ${}^7\text{Be}(p, \gamma){}^8\text{B}$ reaction

F.M. Nunes<sup>1</sup>, R. Crespo<sup>1</sup>, I.J. Thompson<sup>2</sup>

<sup>1</sup> Departamento de Física, CENTRA, IST, Lisboa, Portugal.

<sup>2</sup> Department of Physics, University of Surrey, GU2 5XH, U.K.

## Abstract

Quadrupole and octupole couplings to all bound states of  ${}^7\text{Be}$  are included in describing the capture reaction  ${}^7\text{Be}(p, \gamma){}^8\text{B}$ . We verify, contrary to what we had initially stated, that the energy behaviour of the Astrophysical S-factor in the energy range of interest is not significantly sensitive to the core couplings in the g.s. (g.s.) of  ${}^8\text{B}$  although its overall magnitude is shifted. We find there is some sensitivity to the various deformation models when introducing the nuclear interaction for calculating the scattering states. The various deformation models predict quite different contributions to the quadrupole and magnetic moments but in order to compare with the data the quadrupole and magnetic moment of  ${}^7\text{Be}$  need to be measured.

The importance of reliable extrapolations of the proton capture reactions from the measurable energy range to astrophysical energies is so far unquestionable although experiments have been reaching lower and lower in energy. Up to the present year it was fairly well established that the low energy behaviour of the Astrophysical S-factor was determined by the asymptotic of the g.s. wavefunction and therefore was not dependent on any particular nuclear model [1]. In this letter we reformulate our results of [2] which indicated that core quadrupole couplings in the g.s. of  ${}^8\text{B}$  could introduce modifications in the low energy behaviour of the Astrophysical S-factor. Due to a numerical error this was found not to be correct. We present extended results of calculations including all bound states of the core ( ${}^7\text{Be}$ ) and test the effect of octupole as well as quadrupole couplings. In addition we clarify the role of the scattering nuclear interactions in the evaluation of the S-factors.

For a fair evaluation of the real effect of core deformation, we chose the same radius and diffuseness as Tombrello [3], Robertson [4] and Kim [5]. We use the same spin orbit depth as Kim. The depth of the central interaction is adjusted to reproduce the correct binding energy. The deformation of the  ${}^7\text{Be}$  core is taken to be  $|\beta_2| = 0.5$  which corresponds to a quadrupole moment slightly larger than the value for  ${}^7\text{Li}$  ( $Q = -4.06 \pm 0.08$  e fm<sup>2</sup> [6]). According to microscopic calculations [7, 8] the deformation parameter of  ${}^7\text{Be}$  could actually be larger ( $\beta_2 = 0.6 - 0.7$ ), enhancing the effects. Since there is no experimental indication whether  ${}^7\text{Be}$  is prolate or oblate we have considered both possibilities. We have performed the coupled channel calculations for  $p+{}^7\text{Be}$ , for the case of reorientation only, and when both the  $\frac{1}{2}^-$  state and the  $\frac{7}{2}^-$  state of  ${}^7\text{Be}$  are included. Due to the  ${}^4\text{He}-{}^3\text{He}$  cluster nature of  ${}^7\text{Be}$  one would expect the octupole deformation of the core to be non zero. We have also looked into this possibility. In table 1 we present a range of possible models

to describe this system. The probability of finding the system in some particular channels is presented in that same table. The admixtures become very large when core excited states are included. Inclusion of octupole couplings produces a weak effect, although still reducing the admixture caused by the quadrupole deformation. From all cases we find that both the density distribution and the momentum distribution do not differ significantly from those of the inert core models [2] and the results are summarised in table 2. Core deformation tends to increase the radius which reflects the effective increase of volume of the interaction. We verify that in all cases the rms matter radii predicted are slightly too large [9, 10]. The widths are about twice the FWHM obtained from experiment [11] underlining the need for a proper breakup reaction theory [12]. We verify that each channel of the wavefunction reaches its asymptotic limit for  $r \leq 7$  fm to 0.1%.

The quadrupole moment of  $^8\text{B}$  has been measured [13] ( $|Q| = 6.83 \pm 0.21 \text{ e fm}^2$ ), but the quadrupole moment of  $^7\text{Be}$  is not known. In our model we can calculate the quadrupole contribution  $Q_R$  due to the valence proton. In the single channel model, the coupling of the angular momentum implies  $Q_R = 0$ . Due to the algebra, it is the overlap between  $[p_{3/2} \otimes \frac{3}{2}^-]$  and  $[p_{1/2} \otimes \frac{3}{2}^-]$  channels that basically determines the strength of  $Q_R$ . In table 3 we present the contributions from the valence proton of  $^8\text{B}$  to its quadrupole moment within our set of deformed core models. The final prediction for the  $^8\text{B}$  quadrupole moment relies on the core's quadrupole moment and  $B(E2)$  between the core's bound states, as yet unmeasured. The core contribution is mainly proportional to the probability of the  $[p_{1/2} \otimes \frac{3}{2}^-]$  channel. As an example and in order to quantify the core's contribution, if one takes  $Q(^7\text{Be})$  as predicted by GCM calculations [7] one would need  $\beta_2 \simeq 0.25$  to reproduce  $|Q(^8\text{B})|$  within a reorientation model.

In the same way, the magnetic moment of  $^8\text{B}$  is established [6] ( $\mu = 1.0355 \pm 0.0003 \mu_B$ ) but the magnetic moment of  $^7\text{Be}$  has not been measured. In table 3 we present the contributions of the valence proton to the total magnetic moment of the g.s. of  $^8\text{B}$ . Given the sensitivity of the models to these observables, the measurement of the quadrupole and magnetic moments of  $^7\text{Be}$  is very important.

Reorientation couplings increase the value for the S-factor due to the effective volume increase (radius and diffuseness) caused by deformation (fig.1). When core excitation is introduced, the overall normalisation of the wavefunction is taken from the main g.s. channel into other components that have a more rapid radial decay. One would then expect a reduction of the dipole distribution, and a decrease of the S-factor.

In table 4 we present the  $S_{E1}$  for  $E = 20$  keV and  $E = 100$  KeV, followed by the ratio  $\frac{S(E=20)}{S(E=100)}$  in order to give insight to the energy behaviour. As can be immediately seen all models produce the same energy behaviour for this energy range. Contrary to what we stated in the original paper [2], we conclude that the structure of the core does not alter in a significant way the shape of the energy behaviour of the S-factor. Microscopic models appear to corroborate the same energy dependence [14].

Given that the g.s. wavefunction reaches its asymptotic form for  $r > 7$  fm we have

repeated these calculations introducing a radial cutoff at  $r = 7$  fm and comparing with the full calculations. The results are shown in fig.(2). As expected, we find that the contributions from the interior are not important (of the order of 4%) for  $E \simeq 20$  keV in agreement with [1]. The interior contribution increases rapidly with increasing proton energy.

A plot of the S-factor at  $E = 20$  keV as a function of the deformation parameter is presented in fig.(3). The calculations include only E1 transitions and neglect the nuclear interaction in the scattering calculations. There is a non-linear (nearly quadratic) dependence of  $S(20 \text{ keV})$  with  $\beta_2$  due to the volume increase of the core nucleus. In opposition to this effect there is the reduction of normalisation associated with the main contributing channel  $[p_{3/2} \otimes \frac{3}{2}^-]$ . It is not clear how this behaviour relates to the result obtained in [8] where the S-factor is found to have a linear dependence on the quadrupole moment.

In fig.(4) we show the effect of introducing octupole deformation in the description of the core (as an example we take  $\beta_3 = 0.5$ ). Note that because all core states have the same parity  $\langle \phi_i | \hat{O}_3 | \phi_j \rangle = 0$ , so for this system octupole deformation produces its effects through the quadrupole and hexadecapole form factors. The introduction of the  $\beta_3 \neq 0$  produces an increase in the overall normalisation of the S-factor, which again is partially explained by an increase in the volume of the core ( $R_{ws}$  and  $a_{ws}$  have been kept equal to Kim's parameters) but is also caused by the reduction of the excited core components of the g.s. wavefunction.

So far we have always neglected E2 and M1 effects. In fig.(5) we compare calculations performed for the S-factor including only E1 transitions,  $S_{E1}$ , versus those including E2 and M1 contributions as well,  $S_{tot} = S_{E1} + S_{E2} + S_{M1}$  (not taking into account the nuclear interaction for the scattering states). Although at very low energy there is no contribution other than E1, the E2 and M1 transitions are no longer insignificant at  $E = 0.5$  MeV.

In order to estimate the significance of nuclear interactions in the continuum, we performed calculations assuming that the negative parity continuum states would be subject to the same p-core potential used to obtain the g.s. wavefunction given that nothing is known about their nuclear phase shifts. In table 5 we present  $S_{E1}$  for  $E = 20$  keV and  $E = 500$  keV, followed by the ratio  $R = \frac{S(20)}{S(500)}$  for Kim's model, the reorientation models (both  $\beta_2 = 0.5$  and  $\beta_2 = -0.5$ ), and the excitation models (both  $\beta_2 = 0.5$  and  $\beta_2 = -0.5$ ). The rows with \* correspond to calculations including nuclear phase shifts in the scattering states (same interaction as the g.s. interaction). The nuclear interaction in the continuum can produce up to 15% effect on the low energy behaviour of  $S_{E1}$ . This corresponds to an upper limit for the uncertainty induced by the lack of information for the structure of the negative parity states. In fig.(6) we illustrate the modification in the low energy behaviour of  $S_{E1}$  caused by the nuclear interaction in the continuum for the models that only include the g.s. of the core. In fig.(7) we present the equivalent for the models with core excitation. We point out that when including nuclear phase shifts in the scattering states, there is some sensitivity to the core's shape and structure. This is illustrated in fig.(8) where we compare the low energy  $S_{E1}(E)$  plots for the set of models with the experimental results:

Kim's original model, the reorientation models and the core excitation models. The results shown are from calculations which include nuclear phase shifts but only E1 transitions. We include in fig.(8) two sets of data available in this energy region [15, 16] normalised to the most recent  ${}^7\text{Li}(d,p)$  cross section [17].

In conclusion we have extended calculations for the g.s. of  ${}^8\text{B}$  based on the *core + p* model where the core is allowed to deform and excite. The density distribution and the momentum distribution are not very sensitive to the range of models. The quadrupole and the magnetic moments are strongly dependent on the core's structure but in order to make predictions for  ${}^8\text{B}$  it is important to measure the quadrupole and magnetic moment of the core. We found that the overall normalisation of the S-factor is modified with the core's structure, as well as with the shape of the Woods-Saxon g.s. interaction. In all cases the *shape* of the energy behaviour is not significantly changed. Finally we maintain that the uncertainties associated with the  ${}^7\text{Be}-p$  phase shifts (the negative parity states) introduce an uncertainty ( $< 15\%$ ) into the S-factor energy behaviour.

This work was supported by the JNICT grant PBIC/C/FIS/2155/95 and BIC 1481.

## References

- [1] H.M. Xu, C.A. Gagliardi, R.E. Tribble, A.M. Mukhamedzhanov and N.K. Timofeyuk, Phys. Rev. Lett. **73** (1994) 2027
- [2] F.M. Nunes, R. Crespo, I.J. Thompson, Nucl. Phys. **A 615** (1997) 69
- [3] T.A. Tombrello, Nucl. Phys. **71** (1965) 459
- [4] R.G. Robertson, Phys. Rev. **C 7** (1973) 543
- [5] K.H. Kim, M.H. Park and B.T. Kim, Phys. Rev. **C 35** (1987) 363
- [6] F. Ajzenberg-Selove, Nucl. Phys. **A 490** (1988) 1
- [7] P. Descouvemont and D. Baye, Nucl. Phys. **A 567** (1994) 341
- [8] A. Cs    , K. Langanke, S.E. Koonin and T.D. Shoppa, Phys. Rev. **C 52** (1995) 1130
- [9] I. Tanihata et al., Phys. Letts. **B 206** (1988) 592
- [10] J.S. Al-Khalili and J.A. Tostevin, Phys. Rev. Letts. **76** (1996) 3903
- [11] W. Schwab et al., Z. Phys. **350** (1995) 283
- [12] M.M. Obuti et al., Nucl. Phys. **A 609** (1996) 74
- [13] T. Minamisono et al., Phys. Rev. Lett. **69** (1992) 2058
- [14] E. Kolbe, K. Langanke, H.J. Assenbaum, Phys. Lett. **B 214** (1988) 169
- [15] B.W. Filippone et al., Phys. Rev. Lett. **50** (1983) 412
- [16] W. Kavanagh et al., Bull.Amer. Phys. Soc. **14** (1969) 1209
- [17] F. Strieder et al., Z. Phys. **A 355** (1996) 209

Model	$\beta_2$	$\beta_3$	Core States	$V_{ws}$ (MeV)	$P[p_{3/2} \otimes \frac{3}{2}]$	$P[I = \frac{1}{2}^-]$	$P[I = \frac{7}{2}^-]$
Kim [5]	0.0	0.0	$\frac{3}{2}^-$	-31.768	1.00	0.00	0.00
reo1	0.5	0.0	$\frac{3}{2}^-$	-32.5667	0.57	0.00	0.00
reo2	-0.5	0.0	$\frac{3}{2}^-$	-29.2343	0.94	0.00	0.00
exc1	0.5	0.0	$\frac{3}{2}^-; \frac{1}{2}^-; \frac{7}{2}^-$	-29.9156	0.39	0.03	0.14
exc2	-0.5	0.0	$\frac{3}{2}^-; \frac{1}{2}^-; \frac{7}{2}^-$	-28.5198	0.87	0.09	0.01
oct1	0.5	0.5	$\frac{3}{2}^-; \frac{1}{2}^-; \frac{7}{2}^-$	-30.1736	0.41	0.04	0.13
oct2	-0.5	0.5	$\frac{3}{2}^-; \frac{1}{2}^-; \frac{7}{2}^-$	-28.5003	0.87	0.09	0.01

Table 1: Deformed core models for the g.s. of  $^8\text{B}$ : parameters for the nuclear interaction depth (for the other parameters we use Kim's model:  $V_{so} = -2.06$ ,  $R = 2.95$  fm and  $a = 0.52$  fm), the core's structure and the probabilities for the main channels ( $I$  is the spin of the core).

Model	$\sqrt{\langle r_{valence}^2 \rangle}$ (fm)	$\Gamma$ (MeV/c)
Kim [5]	4.623	158
reo1	4.72	154
reo2	4.78	154
exc1	4.64	158
exc2	4.75	154
oct1	4.76	154
oct2	4.81	150

Table 2: Deformed core models for the g.s. of  $^8\text{B}$ : the valence proton contribution to the predicted r.m.s. matter radius and the momentum distribution width.

Model	$Q_R$ (e fm)	$\mu_R$ ( $\mu_B$ )
Kim [5]	0	2.53
reo1	-7.45	-0.18
reo2	3.78	3.09
exc1	-7.07	-0.62
exc2	2.26	3.08
oct1	-7.52	-0.50
oct2	2.30	3.07

Table 3: Quadrupole and Magnetic moments for the g.s. of  $^8\text{B}$ : contributions from the valence proton.

Model	S(100 keV) (eV b)	S(20 keV) (eV b)	$\frac{S(20)}{S(100)}$
Kim	22.4	23.8	1.06
reo1	23.7	25.2	1.06
reo2	24.5	26.0	1.06
exc1	20.7	22.0	1.06
exc2	22.6	24.1	1.06

Table 4: The S-factors at 20 keV and 100 keV with no nuclear phase shifts (using  $R_{max} = 360$  fm) and the S-factor ratio.

Model	S(500 keV) (eV b)	S(20 keV) (eV b)	$R = \frac{S(20)}{S(500)}$	$\frac{\Delta R}{R}$
Kim	24.4	23.8	0.97	
Kim*	21.4	23.4	1.10	12.4 %
reo1	25.8	25.2	0.98	
reo1*	22.9	24.8	1.09	11.2 %
reo2	26.7	26.0	0.98	
reo2*	22.9	25.5	1.12	14.3 %
exc1	22.5	22.0	0.98	
exc1*	19.5	21.6	1.11	13.4 %
exc2	24.5	24.0	0.98	
exc2*	20.9	23.6	1.13	15.0 %

Table 5: The influence of nuclear phase shifts in the S-factors at 20 keV and 500 keV and the S-factor low-energy behaviour (\* including the nuclear phase shifts in the scattering states).

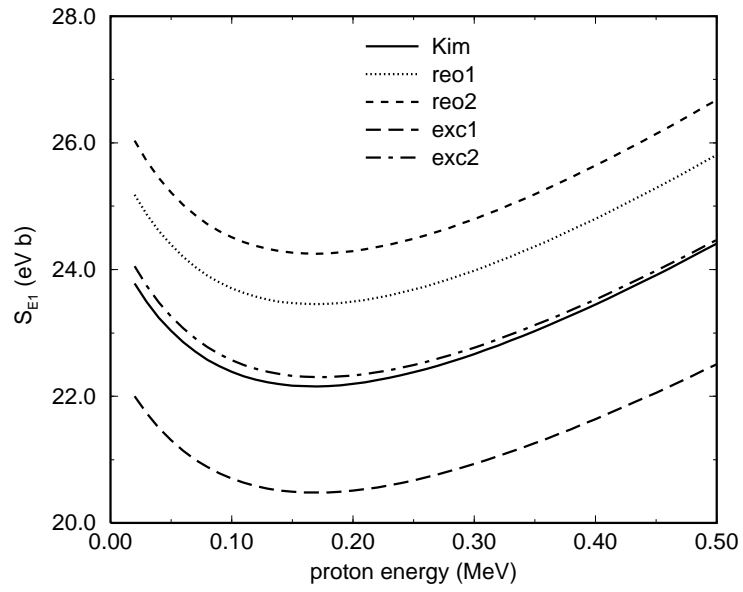


Figure 1: The variation of the  $S(E=20 \text{ keV})$  with the quadrupole deformation parameter.

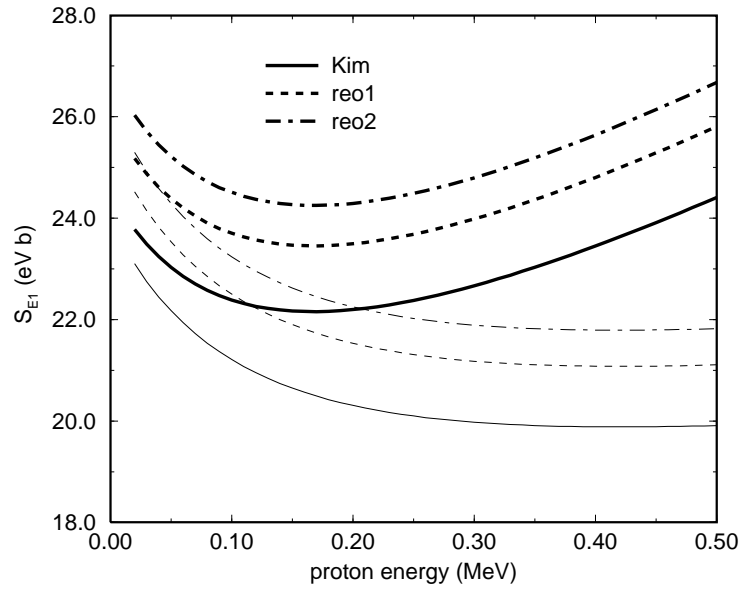


Figure 2: The effect of neglecting the contribution of the interior to the dipole S-factor when neglecting the nuclear interaction in the continuum: the thick lines correspond to the full calculation whereas the thin lines correspond to a radial cutoff of 7 fm.



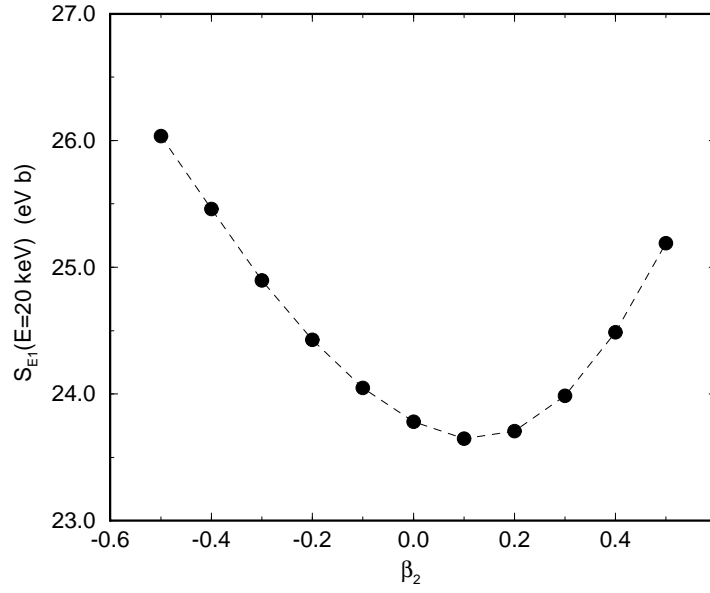


Figure 3: The variation of the  $S(E=20 \text{ keV})$  with the quadrupole deformation parameter.

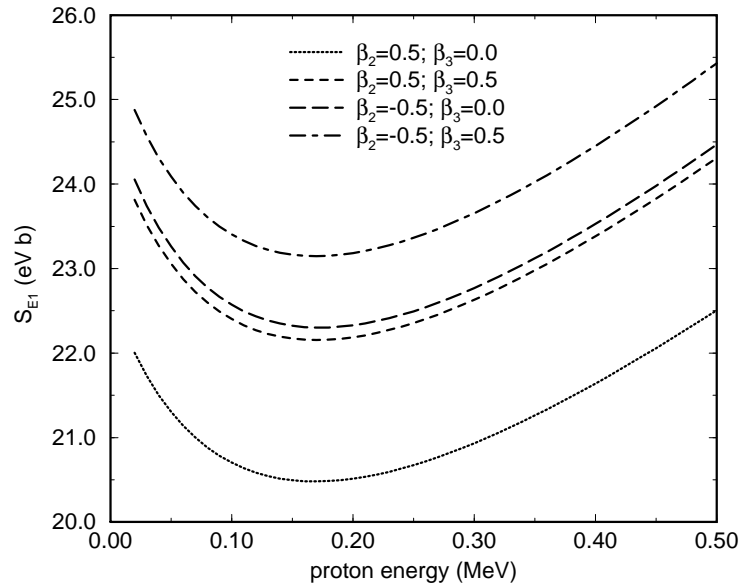


Figure 4: The effect of the octupole couplings on the low energy S-factor.

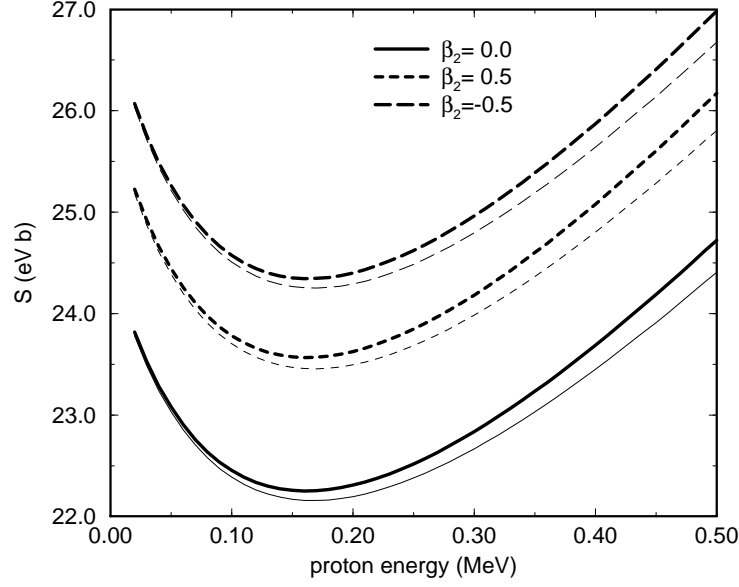


Figure 5: The comparison of  $S_{tot}(E)$  including E1, E2 and M1 transitions (thick lines) and  $S_{E1}(E)$  only due to E1 capture (thin lines).

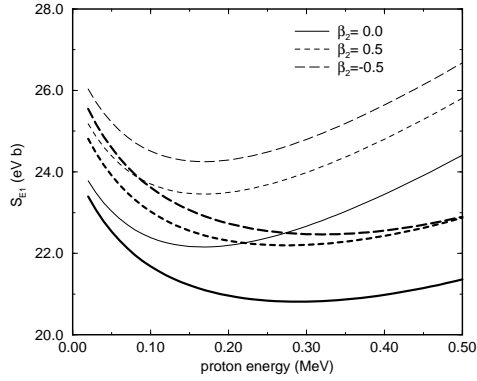


Figure 6: The effect of nuclear phase shifts on the low energy S-factor when considering only reorientation couplings for the g.s. of  ${}^7\text{Be}$ : thick lines include the nuclear interaction for the scattering states.

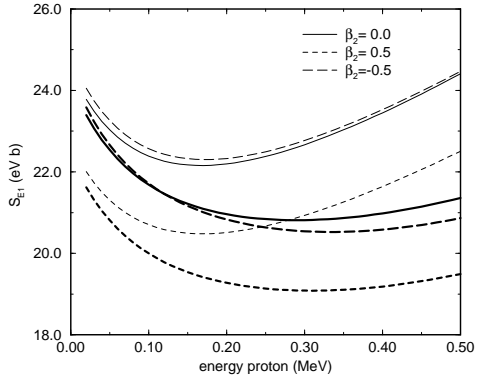


Figure 7: The effect of nuclear phase shifts on the low energy S-factor when considering couplings to excited states of  ${}^7\text{Be}$ : thick lines include the nuclear interaction for the scattering states.

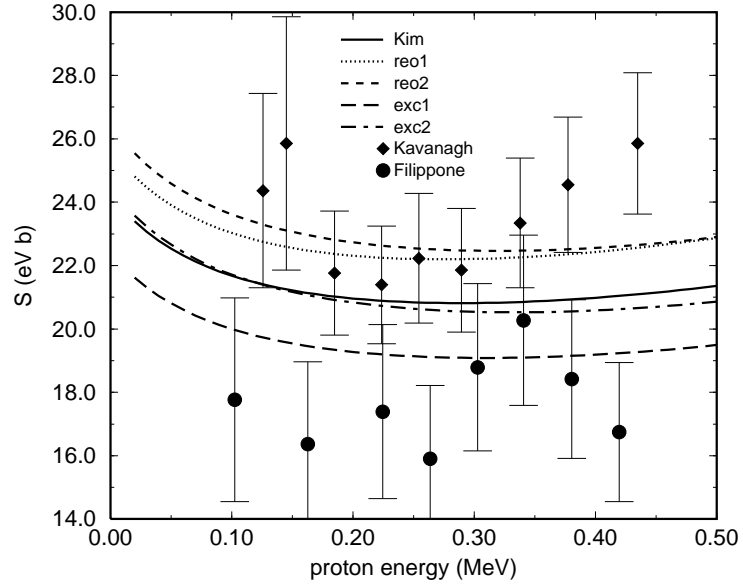


Figure 8: The comparison of  $S_{E1}(E)$  including the nuclear interaction in the scattering states with the low energy data.